

Homogeneous Hydrogenation Catalyzed by Trinuclear Rh^I-Os^{III}-Rh^I Complexes

Peter Comba,^{*,[a]} Andrey Mayboroda,^[a] and Hans Pritzkow^[a]

Keywords: Osmium / Rhodium / Heterometallic complexes / Hydrogenation

Reaction of $[\text{Os}(\text{Hbiim})_2(\text{O}=\text{PPh}_3)_2](\text{NO}_3)$ (H_2biim = 2,2'-biimidazole) with $[\text{RhCl}(\text{cod})]_2$ (cod = 1,5-cyclooctadiene) or $[\text{Rh}(\text{OH})(\text{cod})]_2$ yields biimidazolato-bridged trinuclear Rh^I-Os^{III}-Rh^I complexes, which are highly efficient catalysts for the homogeneous hydrogenation of 1-hexene and cyclohexene. The reactivity of the trinuclear compounds compared with the mononuclear subunits indicates that this is due to

cooperative effects. This is confirmed by spectroscopic and electrochemical data. The solid-state structure of $[\{\text{RhCl}(\text{cod})\}_2(\mu\text{-Hbiim})_2\{\text{Os}(\text{O}=\text{PPh}_3)_2\}](\text{NO}_3)$ was determined by single-crystal X-ray diffraction.

(© Wiley-VCH Verlag GmbH & Co. KGaA, 69451 Weinheim, Germany, 2003)

Introduction

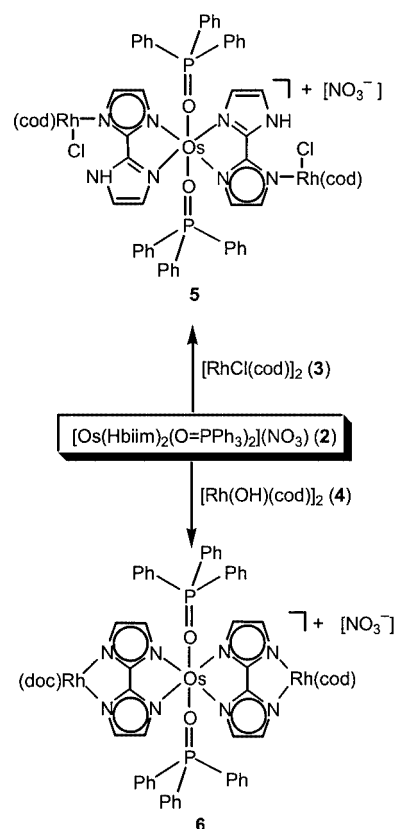
Heterobimetallic complexes are receiving considerable attention in the area of homogeneous catalysis in particular;^[1] the enhanced reactivity of oligonuclear complexes is thought to be due to synergistic effects.^[2–5] For homogeneously catalysed hydrogenation cooperative effects have been reported for some binuclear complexes of platinum-group metals with nitrogen-containing bridging ligands, for example $[\{\text{H}(\text{CO})(\text{PPh}_3)\text{Ru}\}(\mu\text{-pz})_2\{\text{Ir}(\text{TFB})\}]$ (pz = pyrazole; TFB = tetrafluorobenzobicyclo[2.2.2]octadiene)^[4] and $[\{\text{H}(\text{CO})(\text{PPh}_3)\text{Ru}\}(\mu\text{-biim})\{\text{M}(\text{cod})\}]$ (M = Rh, Ir).^[5] Generally, the proposed mechanism involves one catalytically active site; the other metal ion provides this active site with the appropriate environment and has the role of a donor or acceptor of electron density.^[6] The enhanced reactivity is believed to be due to a variation of the ligand field of the active site by the “spectator” chromophore.

2,2'-Biimidazole has been extensively studied as a bridging ligand.^[5,7] The recently reported complex $[\text{Os}(\text{H}_2\text{biim})_2(\text{O}=\text{PPh}_3)_2](\text{NO}_3)_3$ (**1**)^[8] has two 2,2'-biimidazole ligands in the equatorial plane of the octahedral complex and, after deprotonation of the NH sites of 2,2'-biimidazole, transition metal complex fragments can be added. It is therefore a versatile building block for trinuclear complexes.^[8] The use of $[\text{Rh}(\text{cod})]^+$ as such a fragment allowed us to obtain trinuclear Rh^I-Os^{III}-Rh^I compounds. Here, we report the synthesis, characterization and catalytic properties of $[\{\text{RhCl}(\text{cod})\}_2(\mu\text{-Hbiim})_2\{\text{Os}(\text{O}=\text{PPh}_3)_2\}](\text{NO}_3)$ (**5**) and $[\{\text{Rh}(\text{cod})\}_2(\mu\text{-biim})_2\{\text{Os}(\text{O}=\text{PPh}_3)_2\}](\text{NO}_3)$ (**6**).

Result and Discussion

Synthesis and Characterization

The two trinuclear complexes **5** and **6** were obtained from reactions of $[\text{Os}(\text{Hbiim})_2(\text{O}=\text{PPh}_3)_2](\text{NO}_3)$ (**2**)^[8] with $[\text{RhCl}(\text{cod})]_2$ (**3**) and $[\text{Rh}(\text{OH})(\text{cod})]_2$ (**4**), respectively (Scheme 1). The desired products were isolated as red (**5**)



Scheme 1

^[a] Anorganisch-Chemisches Institut, Universität Heidelberg, Im Neuenheimer Feld 270, 69120 Heidelberg, Germany
E-mail: comba@akcomba.oci.uni-heidelberg.de

or brown (**6**) air-stable solids that are insoluble in aromatic and aliphatic hydrocarbons but moderately soluble in dichloromethane and methanol.

Slow evaporation of a solution (dichloromethane/methanol, 4:1, 20 °C) of **5** resulted in single crystals suitable for structural analysis. The geometry of **5**, determined by the analysis of single-crystal X-ray diffraction data, is shown in Figure 1, structural parameters are given in Table 1.

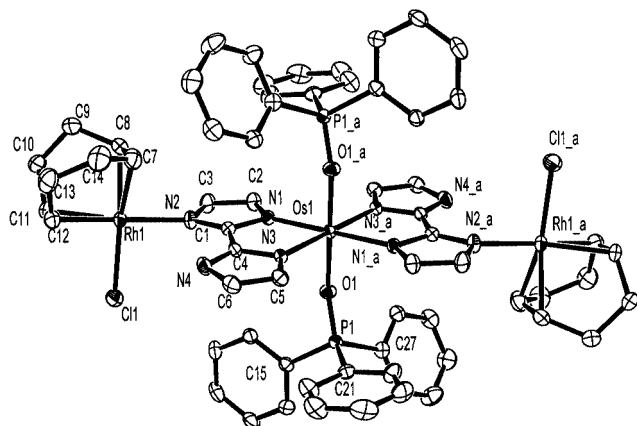


Figure 1. ZORTEP [12] drawing of the complex cation **5**; symmetry transformation used to generate equivalent atoms (a): $-x + 1, -y + 1, -z + 2$

Table 1. Selected geometric parameters of $[\{\text{RhCl}(\text{cod})\}_2(\mu\text{-Hbiim})_2\text{Os}(\text{O}=\text{PPh}_3)_2](\text{NO}_3)\cdot\text{CH}_2\text{Cl}_2$ (**5**)

Bond lengths [Å]	
Os1–O1	2.027(3)
Os1–N1	2.065(4)
Os1–N3	2.080(4)
P1–O1	1.504(3)
C2–C3	1.376(7)
Rh1–N2	2.082(4)
Rh1–C7	2.119(6)
Rh1–C8	2.107(5)
Rh1–C11	2.137(5)
Rh1–C12	2.155(5)
Rh1–Cl1	2.396(2)
Valence angles [°]	
O1–Os1–N1	85.66(14)
O1–Os1–N3	91.93(14)
N1–Os1–N3	77.85(15)
P1–O1–Os1	151.5(2)
N2–Rh1–Cl1	89.92(12)

The coordination sphere of the osmium center is approximately octahedral; the rhodium centers have a square-planar geometry. The Os(1)–N(1) and Os(1)–N(3) distances [2.065(4) and 2.080(4) Å, respectively], are in the range found in related Os^{III} biimidazole^[8] and biimidazolate^[9] complexes. Comparison with the molecular structure of **1**^[8] reveals a distinct difference in the binding of the triphenylphosphane oxide ligand. The Os(1)–O(1) distance in

5 [2.027(3) Å] is somewhat longer than that in **1** [2.012(2) Å], and the P(1)–O(1)–Os(1) angle in **5** [151.5(2)°] is significantly larger than that in **1** [146.53(11)°]. This, together with the EPR spectra (see below), is evidence for significant differences in the electronic structure of the osmium centers between the mononuclear compound **1** and the trinuclear compounds **5** and **6**, and it is an indication of a modification of the electronic properties of the catalytically active rhodium sites.

The EPR spectra (X-band) of **1**, **5** and **6**, recorded in frozen solution [dichloromethane/methanol/tetrahydrofuran (7:1:2), 77 K], are axial, with a large anisotropy;^[10] this is a common observation in EPR spectroscopy of osmium(III) complexes.^[11] The large difference in $\Delta g_{1,2}$ between **1** ($\Delta g_{1,2} = 0.695$) and **5**, **6** ($\Delta g_{1,2} = 1.450, 1.372$) is attributed to the increasing axial distortion (see discussion of the X-ray structural data above) and concomitant changes in the electronic structure.

Electrochemical studies of **2**, **5** and **6** were carried out in methanol at 25 °C; cyclic voltammograms of **2** and **5** are shown in Figure 2. A comparison of the electrochemical behavior of the mononuclear complex **2** with that of the trinuclear compounds **5** and **6** indicates that the deprotonation of 2,2'-biimidazole and formation of the heterotrimetallic complexes results in a significant cathodic shift of the redox potentials of osmium. The Os^{III}/Os^{II} reduction wave, which

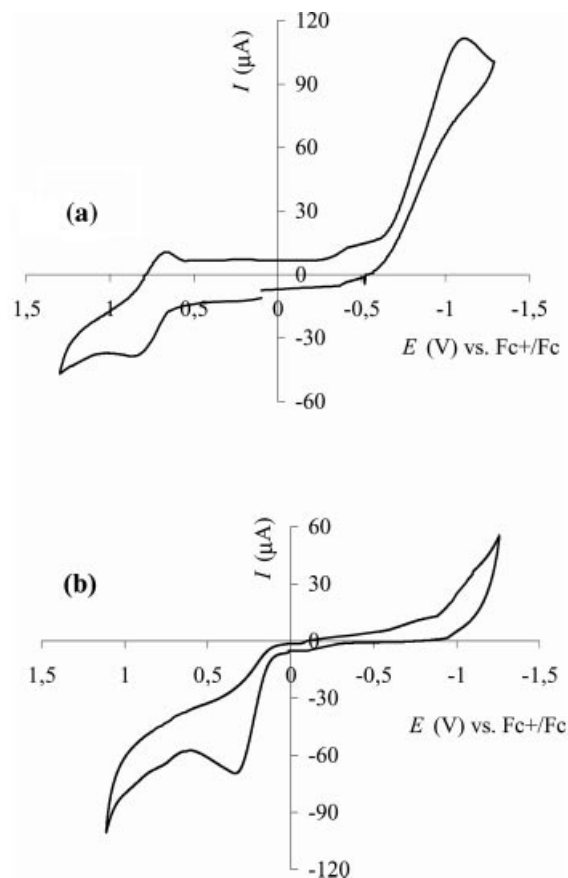


Figure 2. Cyclic voltammograms of: (a) $[\text{Os}(\text{Hbiim})_2(\text{O}=\text{PPh}_3)_2](\text{NO}_3)$ (**2**) and (b) $[\{\text{RhCl}(\text{cod})\}_2(\mu\text{-Hbiim})_2(\text{O}=\text{PPh}_3)_2](\text{NO}_3)$ (**5**)

is observed at -1.14 V for **2**, is beyond the accessible potential range for **5** and **6**. The $\text{Os}^{\text{III}}/\text{Os}^{\text{IV}}$ redox couple was found at $+0.77$ V for **2** and seems to be shifted cathodically for **5** and **6**. These signals are broad and irreversible. The fact that they are not well resolved might be due to overlap of the cyclovoltammetric responses for Os^{III} and Rh^{I} . The oxidation wave of **5** is at $+0.37$ V and that of **6** is at $+0.38$ V. Well-resolved cyclic voltammograms have been reported for biimidazolate-bridged $\text{Pt}^{\text{II}}\text{-Os}^{\text{III}}\text{-Pt}^{\text{II}}$ and $\text{Pd}^{\text{II}}\text{-Os}^{\text{III}}\text{-Pd}^{\text{II}}$ complexes.^[9] Under the same conditions as those reported here the $\text{Os}^{\text{III}}/\text{Os}^{\text{IV}}$ couple was observed at $+0.53$ V for $[\{\text{Pt}(\text{C}_5\text{H}_3(\text{CH}_2\text{NMe}_2\text{-}2,6)_2\})_2\text{Os}(\mu\text{-Hbiim})_2(\text{O}=\text{PPh}_3)_2](\text{NO}_3)(\text{SO}_3\text{SF}_3)_2$ [$\text{C}_5\text{H}_3(\text{CH}_2\text{NMe}_2\text{-}2,6)$ = pincer ligand] and at $+0.23$ V for $[\{\text{Pd}(\text{en})\}_2\text{Os}(\mu\text{-biim})_2(\text{O}=\text{PPh}_3)_2](\text{NO}_3)_3$ (en = ethylene-1,2-diamine).^[9] These observations and interpretations are consistent with a modification of the donor properties of 2,2'-biimidazole due to the deprotonation and coordination to a second metal ion. In agreement with the structural comparison and the EPR spectra, the electrochemical data indicate that the osmium centers in **5** and **6** act as Lewis acids and therefore modify the electronic properties of the catalytically active rhodium sites.

Catalytic Activity

Compounds **5** and **6** catalyze the hydrogenation of 1-hexene and cyclohexene under homogeneous conditions. The results are summarized in Table 2. The reactivities of the mononuclear complexes **1**, **3** and **7** (fragments of **5** and **6**) are included for comparison. The trinuclear complexes **5** and **6** are significantly more active and selective catalysts than the corresponding building blocks **1**, **3** and **7**. The mononuclear osmium complex **1** is almost inactive. This implies that the transformation of the substrate takes place at the rhodium centers of the trinuclear catalysts **5** and **6**. The observation that the mononuclear rhodium complex **7** catalyzes the migration of a double bond in the linear alkene rather than its hydrogenation is interesting. The reduction of 1-hexene in the presence of the trinuclear catalysts **5** and **6** occurs very selectively. The hydrogenation of cyclohexene

is much slower than the reduction of 1-hexene. However, for cyclohexene, the enhancement of the catalytic activity by the trinuclear compounds **5** and **6** is more pronounced. A plausible catalytic pathway includes the hydrogenation of the cyclooctadiene ligand in **5** and **6**, and the formation of a coordinatively unsaturated intermediate by removal of cyclooctane.^[6] The enhancement of the catalytic activity with the trinuclear complexes is due to a modification of the electronic properties of the rhodium centers, and this might occur by electrostatic effects or by electronic communication between the osmium and rhodium centers through the π -conjugated bridging ligand. Catalytic hydrogenation by rhodium complexes usually involves oxidative addition of hydrogen and formation of a π -complex with the alkene, followed by an intramolecular alkene insertion reaction, leading to a Rh-alkyl complex.^[6] The last step is usually rate-determining. A decrease of the electron density on Rh^{I} , due to the Os^{III} center, must lead to a reduction of the energy barrier, and promote the nucleophilic attack of the alkene and formation of Rh-alkyl species. Here, the additional metal center is used as a weak electron acceptor and, therefore, improves the properties of the catalytically active metal ion. The osmium center provides a subtle modification of the electronic structure of rhodium, which promotes the Rh-alkyl complex formation and does not inhibit the oxidative addition of hydrogen.

In summary, we have prepared and characterized trinuclear $\text{Rh}^{\text{I}}\text{-Os}^{\text{III}}\text{-Rh}^{\text{I}}$ complexes with 2,2'-biimidazole as a bridging ligand and shown their utility as catalysts for the homogeneous hydrogenation of 1-hexene and cyclohexene. The significant enhancement of the catalytic activity, relative to the mononuclear building blocks, is believed to be due to a variation of the ligand field induced by the "spectator" metal ion.

Experimental Section

General: $[\text{Os}(\text{H}_2\text{biim})_2(\text{O}=\text{PPh}_3)_2](\text{NO}_3)_3$ (**1**) was prepared by a published procedure.^[8] Its conjugate base $[\text{Os}(\text{Hbiim})_2(\text{O}=\text{PPh}_3)_2](\text{NO}_3)\cdot 2\text{H}_2\text{O}$ (**2**) was obtained by reaction of **1** with KOH

Table 2. Homogeneous hydrogenation^[a] of 1-hexene and cyclohexene in the presence of $[\text{Os}(\text{H}_2\text{biim})_2(\text{O}=\text{PPh}_3)_2](\text{NO}_3)_3$ (**1**), $[\text{RhCl}(\text{cod})]_2$ (**3**), $[\text{Rh}(\text{H}_2\text{biim})(\text{cod})](\text{SO}_3\text{CF}_3)$ (**7**), $[\{\text{RhCl}(\text{cod})\}_2(\mu\text{-Hbiim})_2\{\text{Os}(\text{O}=\text{PPh}_3)_2\}](\text{NO}_3)$ (**5**) and $[\{\text{Rh}(\text{cod})\}_2(\mu\text{-biim})_2\{\text{Os}(\text{O}=\text{PPh}_3)_2\}](\text{NO}_3)$ (**6**)

Catalyst	Cat. [mol %]	Time [h]	Hydrogenation of 1-hexene			Hydrogenation of cyclohexene
			Conversion [%]	Yield of by-products [%]		Conversion [%]
				2-hexene	3-hexene	
1	1	10	11	3	3	0
3	1	5	23	8	7	4
7	2	5	29	49	20	2
5	1	5	67	0	0	46
5	1	10	98	0	0	73
6	1	5	53	5	4	34
6	1	10	94	3	1	66

^[a] Reaction conditions: 5 bar H_2 , solvent: $\text{CH}_2\text{Cl}_2/\text{CH}_3\text{OH}$ (9:1).

in methanol/dichloromethane.^[8] IR spectra (KBr pellets) were recorded on a Perkin–Elmer 16PC RT-IR instrument. UV/Vis spectra were obtained with a Cary 1E spectrophotometer. EPR spectra were recorded with a Bruker ESP300E spectrometer (9.4635 GHz) as approx. $1 \times 10^{-3} \text{ mol} \cdot \text{dm}^{-3}$ frozen (liquid nitrogen temperature) solutions in dichloromethane/methanol/tetrahydrofuran (7:2:1). Electrochemical measurements (CV) were performed in solutions of $[\text{NnBu}_4]\text{PF}_6$ ($0.1 \text{ mol} \cdot \text{dm}^{-3}$) in methanol at 293 K, using a BAS 100B system with a glassy-carbon working electrode, a platinum auxiliary electrode and an Ag/AgCl reference electrode. All potentials are quoted versus the ferrocene/ferrocenium couple ($E = 0.0 \text{ V}$). Mass spectra were recorded on a Finnigan MAT 8230 instrument. GC-MS analyses were performed on a Fison GC 8000/MD 800 series instrument, equipped with a ZB-1 (Zebron) column. Melting (decomposition) points were determined with a Gallenkamp MFB 595 010 M melting point apparatus. Organic solvents (methanol, dichloromethane) were freshly distilled before use. Microanalyses were obtained from the microanalytical laboratory of the chemical institute of the University of Heidelberg.

Catalytic Hydrogenation of 1-Hexene and Cyclohexene: All experiments were performed in a 100 mL stainless steel autoclave with an inner polytetrafluoroethylene vessel. In a typical experiment, 0.016 mmol of the catalyst was placed as a solid in the autoclave, supplied with a magnetic stirrer. Whilst stirring, the catalyst was dissolved in dichloromethane (6 mL) or a mixture of dichloromethane and methanol (90:10). The alkene (0.16 mmol) was then added to the solution of the catalyst. The autoclave was evacuated three times and filled with hydrogen. The pressure of hydrogen was then increased to 5 bar. The reaction mixture was stirred for 5 h. The autoclave was then degassed and all volatile materials were evaporated from the reaction mixture under oil-pump vacuum, and condensed (liquid nitrogen). The resulting solution was analysed by GC-MS.

Synthesis of $[\{\text{RhCl}(\text{cod})\}_2(\mu\text{-Hbiim})_2\{\text{Os}(\text{O}=\text{PPh}_3)_2\}](\text{NO}_3) \cdot \text{CH}_2\text{Cl}_2$ (5): $[\text{Os}(\text{Hbiim})_2(\text{O}=\text{Ph}_3)_2](\text{NO}_3) \cdot 2\text{H}_2\text{O}$ (**2**; 300 mg, 0.27 mmol) was dissolved in a dichloromethane/methanol mixture (4:1, 15 mL) at 25 °C. $[\text{RhCl}(\text{cod})]_2$ (**3**; 0.27 mmol), in methanol (5 mL) was added to the solution. The reaction mixture immediately turned from violet to red. The solution was stirred for 2 h, and the volume of the solution was then reduced to 4 mL. After 10 h red crystals of **5** precipitated. The slurry was decanted and the crystalline precipitate was washed twice with acetone (5 mL) and dried under an oil-pump vacuum to afford **5**. Yield: 290 mg (73% based on **2**). Mp: gradual decomposition above 150 °C. IR (KBr): $\nu(\text{P}=\text{O})$ 1120 cm^{-1} , $\nu_a(\text{NO}_3^-)$ 1332, $\nu(\text{Ar}, \text{C}=\text{C})$ 1438, $\nu(\text{NH})$ 3050. UV/Vis (CH_2Cl_2): λ_{max} = 360 nm ($\epsilon = 7.5 \times 10^3 \text{ mol}^{-1} \cdot \text{dm}^3 \cdot \text{cm}^{-1}$), 541 nm ($\epsilon = 4.7 \times 10^2 \text{ mol}^{-1} \cdot \text{dm}^3 \cdot \text{cm}^{-1}$). CV (CH_3OH , 25 °C): $E_{\text{ox}} = +0.37 \text{ V}$ (irr.). MS (FAB): m/z (%) = 1507 (21) $[\text{C}_{64}\text{H}_{64}\text{N}_8\text{Cl}_2\text{O}_2\text{P}_2\text{OsRh}_2]^+$, 1260 (32) $[\text{C}_{56}\text{H}_{52}\text{N}_8\text{ClO}_2\text{P}_2\text{OsRh}]^+$, 1014 (66) $[\text{C}_{48}\text{H}_{40}\text{N}_8\text{O}_2\text{P}_2\text{Os}]^+$, 736 (100) $[\text{C}_{30}\text{H}_{25}\text{N}_8\text{OPOs}]^+$. $\text{C}_{64}\text{H}_{64}\text{Cl}_2\text{N}_8\text{O}_5\text{P}_2\text{OsRh}_2 \cdot \text{CH}_2\text{Cl}_2$ (1653.03): calcd. C 47.23, H 4.02, N 7.64; found C 46.80, H 4.41, N 7.72.

Synthesis of $[\{\text{Rh}(\text{cod})\}_2(\mu\text{-biim})_2\{\text{Os}(\text{O}=\text{PPh}_3)_2\}](\text{NO}_3)$ (6): $[\text{Os}(\text{Hbiim})_2(\text{O}=\text{Ph}_3)_2](\text{NO}_3) \cdot 2\text{H}_2\text{O}$ (**2**; 300 mg, 0.27 mmol) was treated with $[\text{Rh}(\text{OH})(\text{cod})]_2$ (125 mg, 0.27 mmol) in dichloromethane/methanol (4:1, 20 mL) solution at 25 °C. The reaction mixture was stirred for 2 h and the solvent was then removed under an oil-pump vacuum to afford **6** as a brown solid in quantitative yield. Mp: gradual decomposition above 150 °C. IR (KBr): $\nu(\text{P}=\text{O})$ 1118 cm^{-1} , $\nu_a(\text{NO}_3^-)$ 1332, $\nu(\text{Ar}, \text{C}=\text{C})$ 1436. UV/Vis (CH_2Cl_2): λ_{max} =

349 nm ($\epsilon = 6.3 \times 10^3 \text{ mol}^{-1} \cdot \text{dm}^3 \cdot \text{cm}^{-1}$), 556 nm ($\epsilon = 4.7 \times 10^2 \text{ mol}^{-1} \cdot \text{dm}^3 \cdot \text{cm}^{-1}$). CV (CH_3OH , 25 °C): $E_{\text{ox}} = +0.38 \text{ V}$ (irr.). MS (FAB): m/z (%) = 1434 (100) $[\text{C}_{64}\text{H}_{62}\text{N}_8\text{O}_2\text{P}_2\text{OsRh}_2]^+$, 1224 (28) $[\text{C}_{56}\text{H}_{52}\text{N}_8\text{IO}_2\text{P}_2\text{OsRh}]^+$, 1156 (31) $[\text{C}_{46}\text{H}_{47}\text{N}_8\text{OPOsRh}_2]^+$, 946 (42) $[\text{C}_{38}\text{H}_{35}\text{N}_8\text{OPOsRh}]^+$. $\text{C}_{64}\text{H}_{62}\text{N}_8\text{O}_5\text{OsP}_2\text{Rh}_2$ (1513.3): calcd. C 51.41, H 4.18, N 8.43; found C 51.01, H 4.79, N 8.76.

X-ray Crystallographic Analysis of 5: Crystallized from $\text{CH}_2\text{Cl}_2/\text{MeOH}$, formula $\text{C}_{64}\text{H}_{64}\text{Cl}_2\text{N}_8\text{O}_5\text{OsP}_2\text{Rh}_2$, $M = 1568.13$ ($[\text{C}_{64}\text{H}_{64}\text{Cl}_2\text{N}_8\text{O}_5\text{OsP}_2\text{Rh}_2] \cdot \text{NO}_3$), red crystal $0.28 \times 0.25 \times 0.14 \text{ mm}^3$, triclinic, space group $P\bar{1}$, $a = 10.7225(9)$, $b = 13.3347(11)$, $c = 13.3707(11) \text{ Å}$, $\alpha = 110.312(2)^\circ$, $\beta = 100.589(2)^\circ$, $\gamma = 107.462(2)^\circ$, $Z = 1$, $V = 1619.3(2) \text{ Å}^3$, $\rho_{\text{calcd.}} = 1.682 \text{ g} \cdot \text{cm}^{-3}$, θ scan range $1.77 < \theta < 32.05$, Mo-K α radiation ($\lambda = 0.71073 \text{ Å}$), $T = 103(2) \text{ K}$. 28335 reflections collected, 10965 independent reflections, 8432 observed reflections [$I \geq 2\sigma(I)$], 551 refined parameters, $R = 0.0435$, $wR^2 = 0.1214$, semi-empirical absorption correction from equivalents. Structure was solved by direct methods. Refinement was carried out by full-matrix least-squares techniques on F^2 . Program used: structure solution and refinement: SHELXTL NT5.1 (G. M. Sheldrick, Bruker-AXS, Madison, Wisconsin, USA, 1998) Hydrogen atoms were located from the difference-Fourier map. All hydrogen atoms were fully refined. All non-hydrogen atoms were refined anisotropically.

CCDC-196197 contains the supplementary crystallographic data for this paper. These data can be obtained free of charge at www.ccdc.cam.ac.uk/conts/retrieving.html [or from the Cambridge Crystallographic Data Centre, 12, Union Road, Cambridge CB2 1EZ, UK; Fax: (internat.) +44-1223/336-033; E-mail: deposit@ccdc.cam.ac.uk].

Acknowledgments

Financial support by the Alexander von Humboldt-Stiftung is gratefully acknowledged. We also thank Degussa-Hüls AG for a generous gift of OsO_4 and RhCl_3 .

- [1] [1a] R. Choukroun, D. Gervais, P. Kalck, F. Senocq, *J. Organomet. Chem.* **1987**, 335, C9–C12. [1b] R. Mutin, C. Lucas, J. Thivole-Cazat, V. Dufand, F. Dany, J. M. Basset, *J. Chem. Soc., Chem. Commun.* **1988**, 896–898. [1c] E. Sola, V. I. Bakhmutov, F. Torres, A. Elduque, J. A. Lopez, F. Lahoz, H. Werner, L. A. Oro, *Organometallics* **1998**, 17, 683–696.
- [2] L. Gelmini, D. W. Stephan, *Organometallics* **1988**, 7, 849–855.
- [3] P. Braunstein, X. Morise, *Organometallics* **1998**, 17, 540–550.
- [4] M. A. Esteruelas, M. P. Garcia, A. M. Lopez, L. Oro, *Organometallics* **1991**, 10, 127–133.
- [5] M. P. Garcia, A. M. López, M. A. Esteruelas, F. J. Lahoz, L. A. Oro, *Chem. Commun.* **1988**, 793–795.
- [6] P. A. Chaloner, M. A. Esteruelas, F. João, L. A. Oro, *Homogeneous Hydrogenation*, Kluwer Academic Publishers, Dordrecht, **1993**.
- [7] [7a] S. W. Kaiser, R. B. Saillant, W. M. Butler, P. G. Rasmussen, *Inorg. Chem.* **1976**, 15, 2688–2694. [7b] M. S. Haddad, D. N. Hendrickson, *Inorg. Chem.* **1978**, 17, 2622–2630. [7c] R. Usón, L. A. Oro, J. Gimeno, M. A. Ciriano, J. A. Cabeza, *J. Chem. Soc., Dalton Trans.* **1983**, 233–230. [7d] P. Majumdar, S.-M. Peng, S. Goswami, *J. Chem. Soc., Dalton Trans.* **1998**, 1569–1574. [7e] A. Maiboroda, G. Rheinwald, H. Lang, *Inorg. Chem. Commun.* **2001**, 4, 381–383.
- [8] A. Maiboroda, G. Rheinwald, H. Lang, *Eur. J. Inorg. Chem.* **2001**, 2263–2269.

- ^[9] A. Mayboroda, P. Comba, H. Pritzkow, G. Rheinwald, H. Lang, G. van Koten, *Eur. J. Inorg. Chem.* **2003**, 1703–1710.
- ^[10] EPR spectroscopic data: $g_1 = 2.1755$, $g_2 = 2.8707$ (**1**); $g_1 = 1.9012$, $g_2 = 3.3511$ (**5**); $g_1 = 1.9153$, $g_2 = 3.2871$ (**6**).
- ^[11] ^[11a] R. E. De-Simone, R. S. Drago, *J. Am. Chem. Soc.* **1970**, 92, 2343. ^[11b] G. K. Lahiri, S. Bhattacharya, B. K. Ghosh, A. Chakravorty, *Inorg. Chem.* **1977**, 26, 4324. ^[11c] E. M. Kober, T. J. Mayer, *Inorg. Chem.* **1983**, 22, 1614. ^[11d] K. Majumder, S.-M. Peng, S. Bhattacharya, *J. Chem. Soc., Dalton Trans.* **2001**, 284–288.
- ^[12] L. Zsolnai, G. Huttner, ZORTEP, Program for PC, 1994, University of Heidelberg.

Received April 16, 2003